The American Journal of Pathology, Vol. 180, No. 2, February 2012

DOI: 10.1016/j.ajpath.2011.10.031

Musculoskeletal Pathology

Antibodies against Muscle-Specific Kinase Impair Both Presynaptic and Postsynaptic Functions in a Murine Model of Myasthenia Gravis

Shuuichi Mori,* Sachiho Kubo,* Takuyu Akiyoshi,*† Shigeru Yamada,* Tsuyoshi Miyazaki,* Harumi Hotta,‡ Junzo Desaki,§ Masahiko Kishi,¶ Tetsuro Konishi,‖ Yuri Nishino,**††‡‡ Atsuo Miyazawa,**††‡‡ Naoki Maruyama,§§ and Kazuhiro Shigemoto*

From the Departments of Geriatric Medicine, Autonomic Nervous System,‡ and Molecular Regulation of Aging,§§ Tokyo Metropolitan Institute of Gerontology, Tokyo; the Department of Geriatric Medicine,† Graduate School of Medicine and Faculty of Medicine, the University of Tokyo, Tokyo; the Department of Integrated Basic Medicine Research,§ Ehime University School of Medicine, Ehime; the Department of Internal Medicine,¶ Toho University Sakura Medical Center, Chiba; the Department of Neurology,‖ National Hospital Organization Utano National Hospital, Kyoto; the Bio-Multisome Research Team,** RIKEN SPring-8 Center, Harima Institute, Hyogo; the Graduate School of Life Science,†† University of Hyogo, Hyogo; and Core Research for Evolutional Science and Technology,‡‡ Japan Science and Technology Agency (CREST-JST), Tokyo, Japan*

Antibodies against acetylcholine receptors (AChRs) cause pathogenicity in myasthenia gravis (MG) patients through complement pathway-mediated destruction of postsynaptic membranes at neuromuscular junctions (NMJs). However, antibodies against muscle-specific kinase (MuSK), which constitute a major subclass of antibodies found in MG patients, do not activate the complement pathway. To investigate the pathophysiology of MuSK-MG and establish an experimental autoimmune MG (EAMG) model, we injected MuSK protein into mice deficient in complement component five (C5). MuSK-injected mice simultaneously developed severe muscle weakness, accompanied by an electromyographic pattern such as is typically observed in MG patients. In addition, we observed morphological and functional defects in the NMJs of EAMG mice, demonstrating that complement activation is not necessary for the onset of MuSK-MG. Furthermore, MuSK-injected mice exhibited acetylcholinesterase (AChE) inhibitor-evoked cholinergic hypersensitivity, as is observed in MuSK-MG patients, and a decrease in both AChE and the AChE-anchoring protein collagen Q at postsynaptic membranes. These findings suggest that MuSK is indispensable for the maintenance of NMJ structure and function, and that disruption of MuSK activity by autoantibodies causes MG. This mouse model of EAMG could be used to develop appropriate medications for the treatment of MuSK-MG in humans. ***(Am J Pathol 2012, 180:798–810; DOI: 10.1016/j.ajpath.2011.10.031)***

Myasthenia gravis (MG), the most common disorder of neuromuscular synapses, is caused by autoantibodies against postsynaptic membranes at neuromuscular junctions (NMJs).[1,2] The characteristic clinical features of this autoimmune disease include ptosis, fatigue, and muscular weakness. In 2001, autoantibodies against muscle-specific kinase (MuSK) were found in 70% of patients with generalized MG who lacked antibodies to acetylcholine receptors (AChRs).[3] MuSK, a receptor tyrosine kinase, is concentrated at NMJs from the earliest stages of synaptogenesis and is required for the formation of NMJs during development.[4] Recent studies demonstrated that MuSK is activated by dimerization with low-density lipo-

Supported by grants from the Health Science Research Grants for Research on Psychiatric and Neurological Diseases and Mental Health (H19-Psycho-General-19 to K.S.), Comprehensive Research of Aging and Health (H22-Aging-General-002 to K.S.) from the Ministry of Health, Labor, and Welfare, Japan, Grants-in-Aid for Scientific Research on Innovative Area (21200023 to K.S.), Grants-in-Aid for Scientific Research (C) (21591102 to K.S.), Grants-in-Aid for Young Scientists (B) (23791009 to S.M.) from the Ministry of Education, Science, and Culture, Japan, and Intramural Research Grant (22-5 to K.S.) for Neurological and Psychiatric Disorders of National Center of Neurology and Psychiatry.

Accepted for publication October 25, 2011.

Supplemental material for this article can be found at *http://ajp.amjpathol.org* or at doi: 10.1016/j.ajpath.2011.10.031.

Address reprint requests to Kazuhiro Shigemoto, M.D., Ph.D., Tokyo Metropolitan Institute of Gerontology, Department of Geriatric Medicine, Sakaecho 35-2, Itabashi-ku, Tokyo 173-0015 Japan. E-mail: kazshige@tmig.or.jp.

protein receptor-related protein 4 (LRP4) on agrin binding to LRP4.[5,6]

We previously developed a model of experimental autoimmune myasthenia gravis (EAMG) caused by MuSK antibodies (MuSK Abs) by active immunization of rabbits with recombinant soluble MuSK protein.[7] In addition, passive transfer of human MuSK Abs from MG patients into mice was shown to cause MG.[8] These studies not only demonstrate the pathogenicity of MuSK Abs in the onset of MG, but also suggest that MuSK is required for the maintenance of mature NMJs.

Although previous studies have suggested that the disruption of NMJ maintenance by MuSK Abs might cause MG, several questions remain regarding the pathology of MuSK-MG. First, MuSK Abs in MG patients are mainly composed of the IgG4 subclass.[9,10] IgG4 antibodies do not activate the classical complement pathway, and thus cannot act through the same mechanism observed for AChR antibodies in MG.[2] Additionally, several studies have shown that small amounts of additional complement-fixing subclasses of MuSK and AChR Abs are also detectable in MuSK-MG patients,[9–11] casting doubt on the pathogenicity of MuSK Abs. Therefore, it is essential to determine whether MuSK Abs cause MG without complement activation.

Second, a number of clinical studies have shown that MuSK-MG constitutes a distinct subclass of MG. For example, patients with MuSK-MG are more prone to severe muscle weakness with respiratory crises and eventual atrophy than those with AChR-MG,[12,13] and thus require emergent and aggressive therapies. In addition, although acetylcholinesterase (AChE) inhibitors are often used effectively as symptomatic treatment for AChR-MG,[1,2] MuSK-MG patients frequently either are unresponsive to this treatment or develop cholinergic crises characterized by increasing muscle weakness.[14] A thorough understanding of the unique pathophysiology of MuSK-MG is crucial for the development and assessment of appropriate medications in the future.

To resolve this critical issue, we generated a new animal model in which 100% of mice synchronously develop EAMG after immunization with MuSK protein. This model not only reveals the pathogenic mechanisms involved in MuSK-MG, but also clarifies the role of MuSK at mature NMJs.

Materials and Methods

Preparation of Recombinant MuSK Protein

The fusion protein expression construct, consisting of the rat MuSK ectodomain and a 3′ myc/His-tag sequence, was generated as described previously.[7] 293-F cells were transfected with FreeStyle MAX reagent (Invitrogen) according to the manufacturer's instructions. Secreted recombinant MuSK protein was purified using Ni-Sepharose (GE Healthcare, Piscataway, NJ), pooled, and concentrated. The purity of the recombinant protein was determined by SDS-PAGE with Coomassie blue staining, and the concentration was determined using a Quant-iT assay kit (Invitrogen) with bovine serum albumin as a standard.

Immunization of Mice

All animal procedures used were approved by the Animal Care and Use Committee of Tokyo Metropolitan Geriatric Hospital and Institute of Gerontology. A/WySnJ and C3-deficient mice were obtained from the Jackson Laboratory (Bar Harbor, ME). A/J, B10.A-*H2*^{a}, BALB/c, and C57BL/6 mice were obtained from Japan SLC (Hamamatsu, Japan). DBA/2 and FVB/N mice were obtained from CLEA Japan (Fuji, Japan). All mice were used after 8 weeks of age. On day 0, adult female mice were anesthetized with tribromoethanol and injected subcutaneously in the hind footpads with 20 μg MuSK emulsified with complete Freund's adjuvant. All mice were boosted with 20 μg MuSK emulsified with incomplete Freund's adjuvant on day 14. All C57BL/6J and C3-deficient mice received a third injection of the same dose emulsified with incomplete adjuvant on day 28. Control mice were injected with equal volumes of PBS or equal doses of ovalbumin (OVA) emulsified with adjuvant in the same manner and on the same schedule. For comparison with MuSK-injected mice, A/WySnJ mice were injected with 20 μg AChR protein, which was purified from *Torpedo californica* as described previously[15] and emulsified with adjuvant on days 0, 14, and 42. When antigen-immunized mice exhibited a prominent cervical hump and gait disturbance, they were analyzed for EAMG.

Measurement of Muscle Strength

Forelimb muscle strength was determined by using an MK-380M grip strength meter (Muromachi Kikai, Tokyo, Japan). Mice were allowed to grip the cage lid while being held by the tail, with hindlimbs suspended, and were pulled horizontally until the grip was released. Seven measurements were performed per mouse. The highest and lowest values were discarded, and the average of the five remaining measurements was used for statistical evaluation.

Measurements of Titer and Subclasses of MuSK Antibodies

Wells of ELISA plates were coated with purified rat MuSK (150 ng/well) diluted in Tris-buffered saline. After a washing with 0.1% Tween-20/Tris-buffered saline, plates were blocked with 4% BlockAce (Dainippon Pharmaceutical, Osaka, Japan), then incubated for 3 hours at 37°C with diluted sera (1:1000 in Tris-buffered saline) from MuSK-immunized and preimmune mice. The plates were washed and then incubated for 1 hour at 37°C with HRP-conjugated antibodies against anti-mouse IgG (1:3000 in 0.1% Tween-20/Tris-buffered saline; GE Healthcare), followed by another washing and reaction with a 3,3′,5,5′-tetramethylbenzidine liquid substrate system (Sigma-Aldrich, St. Louis, MO). The colorimetric reaction was stopped by 2 mol/L HCl (2N HCl), and the values of

absorbance at 450 nm were determined as titers of MuSK antibodies. Subclasses of MuSK antibodies were determined using a Mouse Typer sub-isotyping kit (Bio-Rad Laboratories, Hercules, CA) according to the manufacturer's instructions. Only the measurement of IgE was performed by using antibody (Nordic Immunological Laboratories, Eindhoven, The Netherlands) not in the kit. In isotyping analysis, sera from MuSK-immunized mice were diluted 1:3000.

Electromyography

Changes in compound muscle action potential (CMAP) were studied using a PowerLab 4/26 data acquisition system (ADInstruments, Colorado Springs, CO). Mice were anesthetized with tribromoethanol and maintained at 37°C on a thermoregulation device. Paired stimulating electrodes separated by 2 to 3 mm were inserted intramuscularly near the sciatic notch for supramaximal stimulation at 3 Hz. Recording electrodes were inserted in the medial compartment of the gastrocnemius muscle and near the insertion of the Achilles tendon. To isolate stimulus artifacts, a ground electrode was placed between the stimulus and recording electrodes. Decrement was calculated as percent amplitude change between the first and least CMAPs evoked by a train of 10 impulses. If the amplitude of the first CMAP was the least within the measurement, the decrement was designated as 0%. In drug treatment experiments, neostigmine bromide (37.5 μg/kg; Sigma-Aldrich) was given by intraperitoneal injection. A typical mouse weighing 20 g received 100 μL of freshly prepared solution containing 7.5 μg/mL of neostigmine bromide in PBS. After 20 minutes, the effect of drug treatment was evaluated via electromyography (EMG).

In Vitro *Electrophysiology*

Left phrenic nerve and hemi-diaphragm muscle preparations were made after tribromoethanol anesthetization. The muscle specimen was placed in a 1.0-mL chamber filled with Tyrode's solution, which was constantly oxygenized by a gas mixture of 95% O_2/5% CO_2 released close to the fluid surface. Membrane potentials and miniature endplate potentials (MEPPs) were recorded at room temperature (18°C to 22°C) using a glass microelectrode filled with 3 mol/L KCl via a PowerLab 4/26 data acquisition system. To measure evoked endplate potentials (EPPs), μ-conotoxin GIIIB (Peptide Institute, Osaka, Japan) was added to the chamber (1 μmol/L final concentration) to suppress muscle contraction, and the phrenic nerve was stimulated by silver electrodes with supramaximal voltage at 0.7 Hz. Amplitudes of EPPs and MEPPs were standardized to a membrane potential of −75 mV. Quantal content was calculated by applying the values of mean MEPP amplitude, mean EPP amplitude, and membrane potential in the same muscle fiber to a formula reported previously.[16,17] To analyze rate of EPP decay, an exponential function was fitted to the falling phase portion from 80% to 20% of EPP peak value, and the decay time constant (τ) was calculated using the Peak Parameter program in the LabChart software package (version 7.1.2; ADInstruments). The MEPP frequency was calculated from a >1 minute recording in each NMJ. To exclude the effects of μ-conotoxin treatment and nerve stimulation on spontaneous neurotransmission, frequency measurements were performed separately from those of quantal content. Data for ≥10 NMJs were obtained from each normal or MuSK-immunized mouse.

Whole-Mount Staining of NMJs

For quantification of nerve terminals and AChR and AChE staining areas, whole-mount staining of soleus muscles was performed. Soleus muscles were removed and fixed in 1% paraformaldehyde/PBS for 10 minutes at room temperature, rinsed in PBS, and incubated with 0.1 mol/L glycine/PBS. After filleting muscles into several sheets of fibers using microdissection scissors, muscle slices were incubated with either rhodamine or Alexa Fluor 647-conjugated α-bungarotoxin (BTx, 40 nmol/L in PBS; Invitrogen) to label AChRs for 1 hour at room temperature. Muscles were then rinsed in PBS, permeabilized in methanol at −20°C, washed again in PBS for 30 minutes, and blocked for 1 hour in 2% bovine serum albumin/0.3% TritonX-100/PBS. Slices were then incubated overnight at 4°C in a cocktail of primary antibodies diluted in blocking solution. Axons and nerve terminals were labeled with rabbit polyclonal antibodies against neurofilament (1:400; Millipore-Chemicon International, Temecula, CA) and synaptophysin (1:100; Invitrogen).

For quantification of nerve terminals, muscles were incubated only with anti-synaptophysin. Rabbit polyclonal antibody against AChE (1:1000) was generated by Dr. Terrone L. Rosenberry (Mayo Clinic College of Medicine). Antiserum against collagen Q (ColQ, 1:2000) was prepared by injecting Wistar rats with a synthetic peptide corresponding to residues 35 to 51 of the ColQ deduced primary sequence coupled to keyhole limpet hemocyanin. After incubation with primary antibodies, muscles were rinsed three times (20 minutes each) in PBS and incubated overnight at 4°C with either Alexa Fluor 488- or Alexa Fluor 555-conjugated secondary antibodies (1 μg/mL in blocking solution; Invitrogen) corresponding to the hosts of the primary antibodies. After incubation with secondary antibodies, muscles were rinsed three times (20 minutes each) in PBS and flat-mounted in a SlowFade antifade kit (Invitrogen) for confocal microscopic analysis. For quantification of AChR staining intensity, diaphragms were dissected and fixed in 1% paraformaldehyde/PBS for 1 hour at room temperature, rinsed in PBS, and incubated with 0.1 mol/L glycine/PBS. Some pieces of left hemi-diaphragm were incubated overnight at 4°C with Alexa Fluor 488-BTx (40 nmol/L in PBS; Invitrogen). Muscles were then rinsed three times (20 minutes each) in PBS and flat-mounted in the same way as soleus muscles. Confocal images were acquired with a Leica TCS SP5 confocal laser scanning unit, using a 63× glycerin objective on a Leica DMI6000 microscope (Leica Microsystems, Wetzlar, Germany), and images of ≥30 NMJs were acquired from each control or MuSK-immunized

mouse (n = 3 mice/group). For quantification of synaptophysin, AChR and AChE staining areas were quantified on a maximum projection of confocal images with ImageJ software (version 1.42q; NIH, Bethesda, MD). The ImageJ Analyze Particle program was used to quantify the areas of each staining experiment.

Electron Microscopy

After tribromoethanol anesthetization, tibialis anterior muscles were exposed and fixed *in situ* with 4% glutaraldehyde/0.1 mol/L phosphate buffer at pH 7.3 for 5 minutes. Muscles were then dissected, cut into small strips, postfixed with the same solution for 2 hours at room temperature, rinsed several times in distilled water, and further postfixed with 1% unbuffered osmium tetroxide for 30 minutes. For SEM observation, muscles were treated with a HCl-hydrolysis procedure to remove intramuscular connective tissues as described previously.[18] After a drying via the critical point method and then a sputter coating with platinum, specimens were examined in a Hitachi S-800 SEM (Hitachi High-Technologies, Tokyo, Japan). For TEM observation, diaphragms were fixed *in situ* by injecting the fixative intrathoracically and intraperitoneally until these cavities were filled. Small pieces of fixed muscle were block-stained with 3% aqueous uranyl acetate for 2 hours and embedded in Epon 812 resin (Nissin EM, Tokyo, Japan) after dehydration through an ethanol series. Ultrathin sections were cut with an Ultracut E ultramicrotome (Reichert-Jung, Austria), doubly stained with uranyl acetate and lead citrate, and then examined with a Hitachi HU-12A transmission microscope (Hitachi High-Technologies). For morphometric analysis, TEM images were scanned and the density of junctional folds was determined by the number of folds divided by the length of the presynaptic membrane using ImageJ software (version 1.42q). Images of $\geq$10 NMJs from each mouse were obtained for quantification.

Preparation of IgG Fractions and Fab Fragments from MuSK Antisera

Sera from MG-affected mice were collected, and the IgG fraction was purified with Protein G-Sepharose (GE Healthcare) as anti-MuSK IgG. Fab fragments of anti-MuSK IgG were prepared using a Pierce mouse IgG1 Fab preparation kit (Thermo Scientific, Rockford, IL) with papain digestion. As a control, IgG fractions (normal IgG) and Fab fragments (normal Fab) were prepared from sera of preimmune mice using the same method.

AChR Clustering Assay

The C2C12 cell line was obtained from the American Type Culture Collection (ATCC, Manassas, VA) and used for three to eight passages. Cells were cultured in 12-well plates as myoblasts in 10% fetal calf serum (FCS)/Dulbecco's modified Eagle's medium. When the cells reached confluency, myotube formation was induced by replacing the medium with 2% horse serum/Dulbecco's modified Eagle's medium. The cells were incubated for 3 days, with fresh medium exchange every day, until full differentiation into multinucleated myotubes was observed morphologically. Preparation of recombinant agrin protein was as described previously.[7] Myotubes were treated with 10 μg/mL anti-MuSK IgG or Fab for 30 minutes, and then incubated for 16 hours with 1 nmol/L agrin. AChR clustering was visualized after incubation with 40 nmol/L Alexa Fluor 594-BTx (Invitrogen) in fusion medium for 1 hour at 37°C before fixation. Fluorescence images of myotubes were acquired using a 20$\times$ objective on a Leica DMI6000 microscope; the number of AChR clusters in six randomly selected fields was counted.

MuSK Phosphorylation Assay

The C2C12 myotubes were treated with either 10 μg/mL anti-MuSK IgG or Fab. After 30 minutes, half of the myotube cultures were further treated for 30 minutes with 1 nmol/L agrin, and the remaining cultures were left untreated. The myotubes were lysed and solubilized using a protease inhibitor cocktail (complete EDTA-free; Roche Applied Science, Indianapolis, IN) with 2 mmol/L sodium orthovanadate. Extracts were immunoprecipitated with antibodies directed against MuSK, and the resulting precipitates were immunoblotted with either a mixture of the anti-phosphotyrosine antibodies 4G10 (Millipore, Billerica, MA) and PY20 (Millipore-Chemicon International) or MuSK antibodies. Antibodies directed against MuSK were generated in rabbits as described previously.[7] Band intensities of immunoblots were assessed using ImageJ software (version 1.42q).

Statistical Analysis

Significant differences between control and MuSK-injected mice were analyzed by unpaired t-test. Paired t-test was used to analyze the effect of neostigmine treatment in EMG experiments. Analysis of variance was used to assess AChR clustering and MuSK phosphorylation assays. P values of <0.05 were considered statistically significant.

Results

MuSK Protein Injection Results in Synchronous Muscle Weakness with Weight Loss

A/WySnJ mice were injected with 20 μg of MuSK protein on days 0 and 14 of the experiment. Because A/WySnJ mice carry mutations that result in C5 deficiency,[19] these mice cannot generate a lytic membrane attack complex and are therefore highly resistant to EAMG after AChR immunization.[20,21] All mice (n = 18) injected with MuSK manifested severe muscle weakness with tremors within 2 weeks of the second injection. These symptoms occurred synchronously in all animals, along with the appearance of a prominent cervicothoracic hump, indicat-

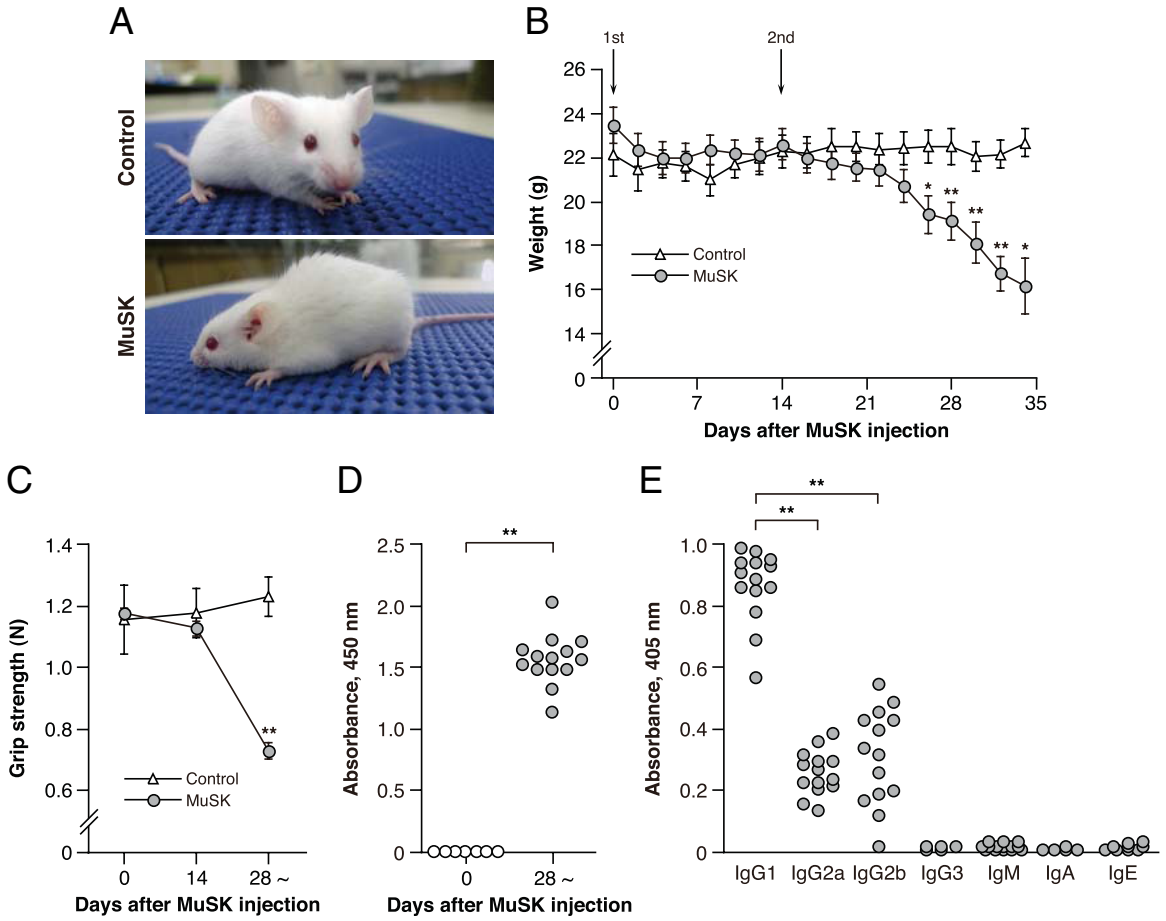

Figure 1. Manifestation of MG-like phenotypes after MuSK injection of A/WySnJ mice. **A:** A/WySnJ mice injected with MuSK protein exhibited a prominent cervical hump and were unable to raise their heads. Control mice injected with vehicle showed no such malformation. MuSK-injected mice lost weight (**B**) and muscle strength (**C**) after the second injection, compared with control mice. Significant weight reduction was observed in MuSK-injected mice at day 26 after the first injection. $n = 5$, control; $n = 18$, MuSK-injected. Data are reported as means ± SEM. $^{*}P < 0.05$; $^{**}P < 0.01$ versus control A/WySnJ mice (*t*-test). **D:** Change in MuSK immunoreactivities of sera after MuSK immunization. Sera from MG-affected mice contained a high titer of MuSK Abs. Sera were prediluted 1:1000 for assay. Values of absorbance at 450 nm were determined as MuSK immunoreactivity. $^{**}P < 0.01$ versus preimmune sera (*t*-test). **E:** Isotyping analysis of MuSK Abs. MuSK Abs were predominantly of the IgG1 subclass, with small amounts of IgG2a and IgG2b, but no detectable IgG3, IgM, IgA, or IgE. Sera were prediluted 1:3000 for assay. Values of absorbance at 405 nm were determined as amounts of MuSK Ab subclasses. $^{**}P < 0.01$ versus IgG1 subclass (analysis of variance). Open symbols, control; filled symbols, MuSK.

ing weak cervical extensor muscles (Figure 1A). In addition, MuSK-injected mice exhibited significant weight loss and muscle weakness (Figure 1, B and C). By contrast, neither vehicle-injected mice ($n = 5$; Figure 1, B and C) nor OVA-injected mice ($n = 5$; data not shown) exhibited weight loss or muscle weakness. We also injected three A/WySnJ mice with *Torpedo californica* AChR protein three times (at days 0, 14, and 42) and found no effect on body weight or muscle strength in these mice (data not shown).

IgG1 Is a Predominant Subclass in MuSK Abs

To test whether muscle weakness of the mice correlates with serum titers of MuSK protein, we used ELISA. Anti-MuSK IgG antibodies were detectable in all MuSK-injected mice, whereas control mice ($n = 5$) had no detectable antibodies to MuSK, which was similar to the preimmune sera (Figure 1D). Isotyping analysis revealed that MuSK Abs were predominantly of the IgG1 subclass, along with smaller amounts of IgG2a and IgG2b (Figure 1E). No other subclasses tested were detected in the MuSK Abs. Mouse IgG1 has functional similarities with human IgG4 in terms of electrophoretic mobility and T-helper type 2 dependency for production.[22] Thus, MuSK-MG in patients and in A/WySnJ mice seems to share a common immune regulatory pathway.

MuSK Abs Change Both Presynaptic and Postsynaptic Structures

To assess directly whether the presence of MuSK Abs results in NMJ structural changes, whole mounts of soleus muscles from MuSK-injected and control mice were double-labeled with BTx (a probe for AChRs), as well as a cocktail of antibodies against neurofilaments and the synaptic vesicle marker synaptophysin (markers for motor neuron axons and terminals, respectively). Extended-focus images collected by confocal microscopy

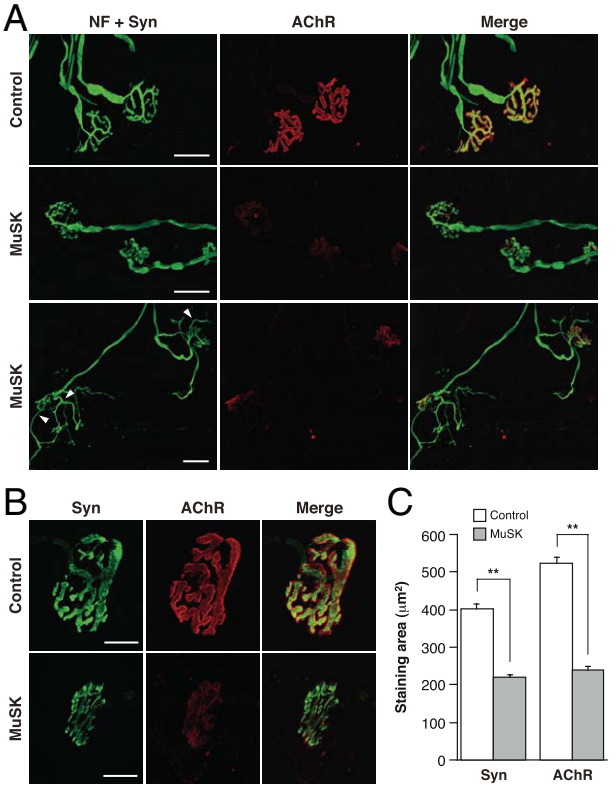

Figure 2. Disorganization of both presynaptic and postsynaptic structures in MuSK-injected mice. **A:** Whole-mount staining of NMJs from soleus muscles. Axons and nerve terminals (green) were stained with anti-neurofilament and anti-synaptophysin antibodies (NF + Syn), and AChRs (red) were labeled with rhodamine-BTx. Some NMJs with axon sprouts were observed in MuSK-injected mice (**arrowheads**). Scale bars: 30 μm. **B:** Soleus muscle nerve terminals were stained with anti-synaptophysin (green) and AChRs were stained with rhodamine-BTx (red). **C:** Synaptophysin and rhodamine-BTx-stained areas decreased to 54.8% and 45.6% of control levels, respectively, in MuSK-injected mice. Scale bars: 20 μm. Data are expressed as means ± SEM from ≥30 NMJs of each mouse (n = 3 mice/group). $^{**}P < 0.01$ versus control (t-test).

were recorded and used for quantitative structural analysis. Accordingly, areas of AChR-clustering and of apposing nerve terminals of NMJs were significantly smaller in soleus muscles of MuSK-injected mice (n = 109 NMJs from three mice), compared with controls (n = 126 NMJs from three mice) (Figure 2, A–C). Furthermore, the density of AChR clustering at NMJ postsynaptic membranes was reduced in soleus and other muscles of MuSK-injected mice, compared with control mice, as evidenced by the intensity of BTx at NMJs (Figure 2, A and B). In addition, axon sprouting, with or without the remnants of nerve terminals, was prominent at the NMJs of MuSK-injected mice (Figure 2A). These results are consistent with the axon outgrowth and reduced AChR clustering observed in other animal models of MuSK-MG.[8,23,24] These results also indicate that MuSK is required by mature NMJs for maintenance of AChR clustering at the postsynaptic membrane and apposing motor terminals. Because MuSK is expressed in skeletal muscle but not in motor neurons,[25] MuSK likely acts via retrograde signals to affect presynaptic NMJ structures.

Changes in Three-Dimensional Structures of the NMJ Subneural Apparatus

Using SEM, we studied the three-dimensional organization of the subneural apparatus at NMJs in tibialis anterior muscles after removing presynaptic terminals and connective tissues.[18] In control mice, the subneural apparatus consisted of complex labyrinthine postsynaptic gutters, approximately 0.9 to 2.8 μm in width, containing numerous slit-like junctional folds. In MuSK-injected mice, however, the subneural apparatus had shallow gutters and lost both labyrinthine structures and formerly prominent slit-like junctional folds (Figure 3A). TEM observations made in diaphragm muscles revealed that synaptic folds underneath motor terminals underwent a pronounced loss in MuSK-injected NMJs, compared with control mice (Figure 3, B and C). Of note, the synaptic membrane was well preserved in MuSK-injected animals (Figure 3B), and we observed no complement-mediated destruction of synaptic structures.[26] These data indicate that MuSK is required for the maintenance of the subneural apparatus and that the reduction of synaptic folds in MuSK-injected mice likely impaired synaptic transmission and caused muscle weakness in these animals.

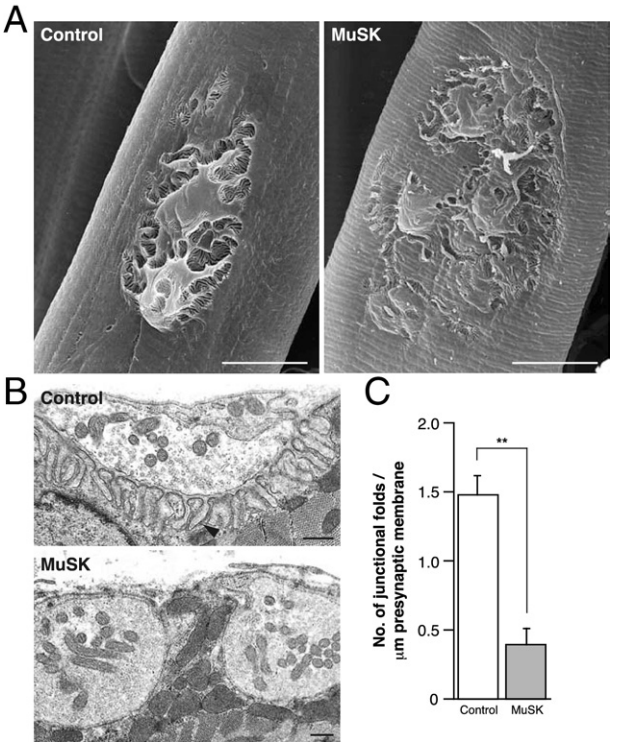

Figure 3. Disruption of NMJ ultrastructure in MuSK-injected mice. **A:** Complex synaptic gutters containing numerous slit-like junctional folds were observed by SEM in NMJs of control tibialis anterior muscle. Synaptic gutter flattening and a decreased number of slit-like junctional folds were observed in NMJs of MuSK-injected mice. Scale bars: 15 μm. **B:** Evenly distributed junctional folds (**arrowhead**) of comparable depth were observed in controls via TEM. Loss of junctional folds was observed in MuSK-injected mice. Scale bars: 500 nm. **C:** Junctional fold densities were significantly decreased in MuSK-injected mice. Data are expressed as means ± SEM from ≥10 NMJs of each mouse (n = 3 mice/group). $^{**}P < 0.01$ versus controls (t-test).

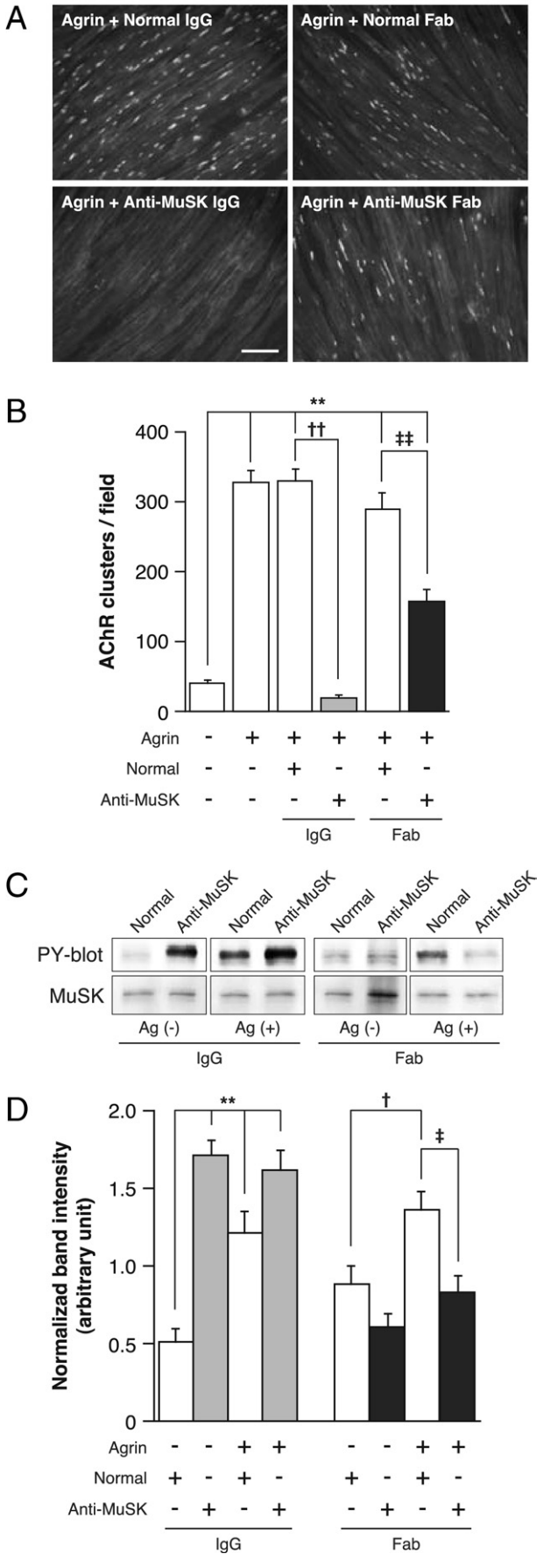

Both Divalent and Monovalent MuSK IgG Perturb MuSK Signaling in C2C12 Myotubes

Because our histological studies demonstrated that MuSK Abs caused EAMG without complement activation, we next tested MuSK Abs in sera from MuSK-injected mice for the ability to interfere with MuSK function *in vitro*. Agrin has been shown to induce the clustering of AChRs in C2C12 myotubes after autophosphorylation by MuSK.[27] When agrin and purified IgG antibodies from the sera of MuSK-injected mice were added to C2C12 myotubes, there was a significant reduction in the marked AChR clustering observed in the presence of purified IgG antibodies from normal sera (Figure 4, A and B). Because inhibition of MuSK signaling by MuSK Abs might have inhibited AChR clustering on C2C12 cells, we analyzed the effect of these antibodies on MuSK phosphorylation. However, MuSK-IgG antibodies induced tyrosine phosphorylation of MuSK in the absence of agrin, and these antibodies did not inhibit activation by agrin (Figure 4, C and D), as described previously,[7,28] suggesting that the divalent MuSK Abs altered a downstream pathway instead of inhibiting MuSK signaling directly.

Next, we generated monovalent Fab fragments of MuSK-IgG antibodies by papain digestion to determine whether they were sufficient to block MuSK signaling in C2C12 cells. Although monovalent Fab fragments of MuSK-IgG antibodies did not activate autophosphorylation of MuSK in the absence of agrin (Figure 4, C and D), these Fab fragments significantly inhibited agrin-induced AChR clustering and MuSK phosphorylation (Figure 4, A–C). These results indicate that monovalent MuSK Abs can block MuSK function *in vitro*.

Neuromuscular Transmission Is Impaired in MuSK-Injected Mice

We performed electrophysiology experiments to determine the effect of MuSK Abs on neuromuscular transmission in mature NMJs. First, we performed EMG experiments in the gastrocnemius muscles of MuSK-injected

Figure 4. Inhibition of agrin-induced MuSK function in cultured myotubes by anti-MuSK IgG and Fab fragments. **A:** C2C12 myotubes were treated with either normal IgG/Fab (10 μg/mL) or anti-MuSK IgG/Fab (10 μg/mL) for 30 minutes and then were incubated with 1 nmol/L agrin for 16 hours. AChR clusters were labeled with Alexa Fluor 594-BTx. Scale bar = 100 μm. **B:** The number of AChR clusters decreased significantly in anti-MuSK IgG or Fab-treated myotubes. Quantification was performed on six randomly selected fields from each of four experiments, and data are expressed as means ± SEM. $^{**}P < 0.01$ versus no treatment; $^{\dagger\dagger}P < 0.01$ versus treatment with agrin + normal IgG; $^{\ddagger\ddagger}P < 0.01$ versus treatment with agrin + normal Fab (analysis of variance). **C:** C2C12 myotubes were treated with either normal IgG/Fab or anti-MuSK IgG/Fab for 30 minutes. Half of the myotube cultures were then treated with 1 nmol/L agrin (Ag) for 30 minutes. Cell extracts were immunoprecipitated with MuSK antibody and immunoblotted with anti-phosphotyrosine (PY-blot) and anti-MuSK. **D:** Divalent anti-MuSK IgG treatment induced MuSK phosphorylation in the absence of agrin, but treatment with monovalent anti-MuSK Fab significantly inhibited agrin-induced MuSK phosphorylation. Band intensities of the PY-blot were normalized to total MuSK. Data are expressed as means ± SEM from three experiments. $^{**}P < 0.01$ versus treatment with normal IgG; $^{\dagger}P < 0.05$ versus treatment with normal Fab; $^{\ddagger}P < 0.05$ versus treatment with agrin + normal Fab (analysis of variance). Control: open symbols; MuSK: filled symbols.

mice with severe muscle weakness. Repetitive stimulation at 3 Hz elicited a declining CMAP response reminiscent of that observed in MG patients, whereas the CMAPs of control mice exhibited no such decline in response (Figure 5A). CMAP amplitude declined by an average of 25.8 ± 3.2% (n = 10) in MuSK-injected mice (Figure 5B). These results indicate that a failure of neuromuscular transmission was the likely cause of muscle weakness in MuSK-injected mice.

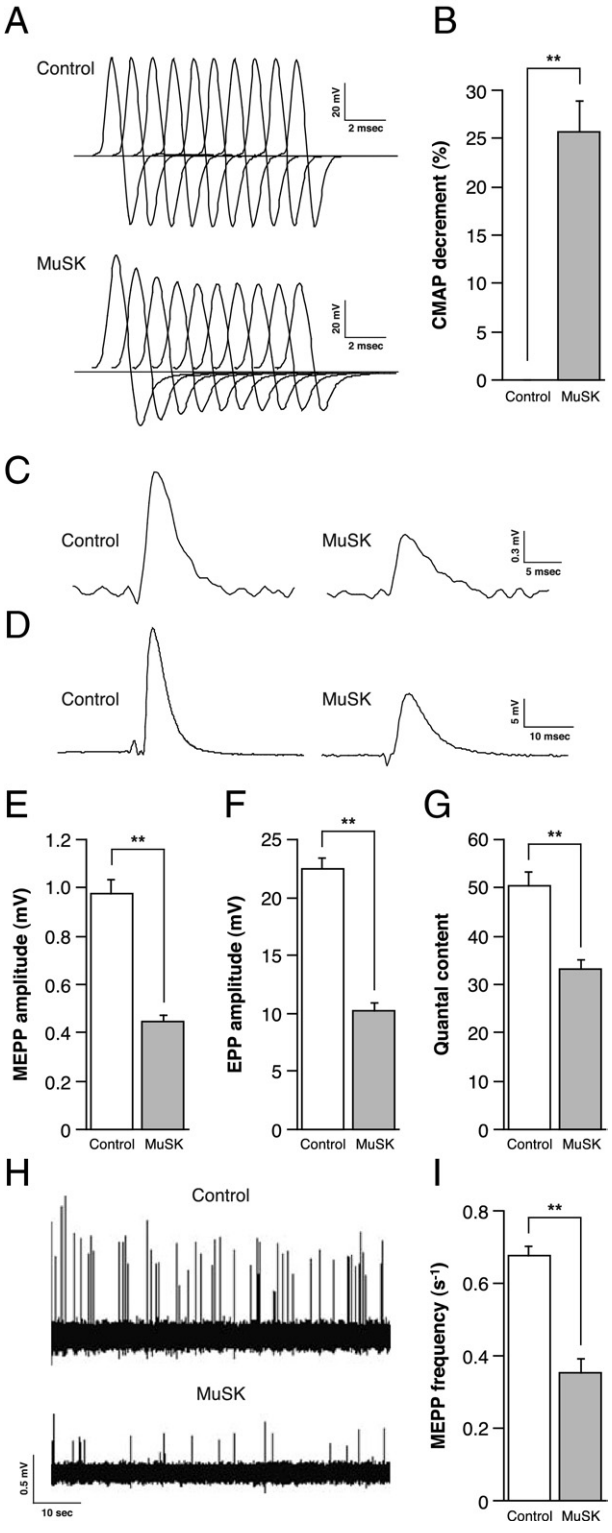

Next, we analyzed the MEPPs and EPPs of MuSK-injected mice via intracellular recordings from muscle fibers of excised hemi-diaphragms.[17,29] No significant difference was observed in resting membrane potential between control mice (−64.1 ± 0.96 mV) and MuSK-injected mice (−65.4 ± 1.33 mV). In MuSK-injected mice, both MEPP and EPP amplitudes (MEPP, 0.45 ± 0.03 mV; EPP, 10.2 ± 0.67 mV; n = 47 NMJs in 4 mice) were significantly decreased, compared with controls (MEPP, 0.98 ± 0.06 mV; EPP, 22.4 ± 0.92 mV; n = 63 NMJs in 3 mice) (Figure 5, C–F). A decrease in EPP amplitude could result either from fewer transmitter quanta being released by a single nerve impulse or from a smaller effect of individual quanta.[30] In addition to the decreased MEPP amplitude, which indicates a smaller postsynaptic effect, the mean quantal content (ie, the steady-state number of quanta released by a single nerve impulse under stimulation at 0.7 Hz) of MuSK-injected diaphragms was also decreased, falling to 33.3 ± 1.78 (or 66.2% of the normal value, 50.3 ± 2.92) (Figure 5G). Taken together, these two effects could result in decreased EPP amplitude, leading to CMAP amplitude decrements.

In addition to the decrease in stimulation-dependent quantal release, MuSK-injected mice (0.35 ± 0.04/s; n = 48 NMJs in 4 mice) exhibited a 52% reduction in spontaneous release, as observed in MEPP frequency, compared with controls (0.67 ± 0.02/s; n = 61 NMJs in 4 mice) (Figure 5, H and I). Because MuSK protein injection resulted in decrease in MEPP amplitude due to the loss of AChR clusters, we could not exclude the possibility that some of the emerging MEPPs were undetectable by our method. However, these results might indicate a low probability of spontaneous quantal ACh release resulting from a presynaptic defect in MuSK-injected mice, as described previously.[31,32]

MuSK-EAMG Is Inducible in Other Complement-Deficient Strains of Mice

A/WySnJ mice exhibit a significant loss of mature B cells due to the B-cell maturation defect-1 (*Bcmd*-1) mutant allele of B-cell-activating factor receptor (*BAFF-R*), and are genetically prone to develop B cell-mediated autoimmunity.[33,34] [*BAFF-R* has since been reclassified as tumor necrosis factor receptor superfamily, member 13c

Figure 5. Impairment of neuromuscular transmission after MuSK injection. **A:** Representative EMG traces during repetitive nerve stimulation. MuSK-injected mice exhibited a decremental CMAP amplitude response, consistent with MG. **B:** MuSK-injected mice exhibited significant CMAP decline (mean, 25.8 ± 3.2%). n = 3, control; n = 10, MuSK-injected. Representative MEPP (**C**) and EPP (**D**) traces from diaphragm muscles. Mean amplitudes of both MEPPs (**E**) and EPPs (**F**), as well as mean quantal release by nerve stimulation (**G**), were decreased in MuSK-injected mice to 45.9%, 45.5%, and 66.2% of control values, respectively. Data are expressed as means ± SEM from ≥10 NMJs of each mouse (n = 3, control; n = 4, MuSK-injected). **H:** Representative MEPP recordings from diaphragm muscles. **I:** MEPP frequencies were decreased to 52.0% of control levels in MuSK-injected mice. Data are expressed as means ± SEM from ≥10 NMJs of each mouse (n = 4 mice/group). $^{**}P < 0.01$ versus controls (t-test).

Table 1. Incidence of MuSK-MG in Seven Mouse Strains

Strain	Total number of mice	MG symptoms (no. of mice)			Incidence (%)
		No symptoms	>10% CMAP decrement		
			<20% weight loss	>20% weight loss	
A/WySnJ	18	0	0	18	100
A/J	5	0	0	5	100
DBA/2	5	0	1	4	100
FVB/N	5	0	0	5	100
B10.A-*H2*^{a}	4	0	4	0	100
BALB/c	4	1	1	2	75.0
C57BL/6	11	6	4	1	45.5

CMAP, compound muscle action potential.

(*Tnfrsf13c*)]. To determine whether the presence of this mutant allele affects the onset of MuSK-EAMG regardless of C5 deficiency, several strains of mice carrying no *Bcmd-1* mutant allele (A/J, DBA/2, FVB/N), but exhibiting the same C5 deficiency as A/WySnJ,[19] were injected with MuSK protein in the same manner and on the same schedule. Almost all of the mice tested exhibited a marked decrease in body weight in addition to impairment of neuromuscular transmission, indicating that a severe form of MuSK-EAMG is inducible in other C5-deficient strains at high incidence (Table 1). Of note, these mice were more sensitive to the onset of MuSK-EAMG than were complement-sufficient mice, such as B10.A-*H2*^{a}, BALB/c, and C57BL/6. Notably, approximately one half of the C57BL/6 mice examined exhibited neither significant weight loss nor neuromuscular transmission defect, despite receiving three injections (Table 1). These results imply that C5-deficient strains may share the genetic background that confers susceptibility to severe MuSK-EAMG.

To validate the results obtained using A/WySnJ mice, genetically engineered C3-deficient mice were used to induce MuSK-EAMG.[35] Although two out of five MuSK-injected mice exhibited moderate (<20%) weight reduction 2 weeks after the third injection (see Supplemental Figure S1 at *http://ajp.amjpathol.org*), these mice exhibited a significant decrease in muscle strength, compared with controls. In addition, all MuSK-injected mice exhibited a decremental CMAP amplitude response after repetitive nerve stimulation, indicating that neuromuscular transmission was impaired (see Supplemental Figure S1, D and E, at *http://ajp.amjpathol.org*). In whole-mount staining of soleus muscles from MuSK-injected mice, the pretzel-like structures of AChR clusters were totally disassembled, and axon sprouting was observed in many NMJs (see Supplemental Figure S1F at *http://ajp.amjpathol.org*). Taken together, these results are consistent with those obtained from A/WySnJ mice, confirming that complement activation is dispensable for the onset of MuSK-EAMG.

MuSK Abs Impair AChE Function at NMJs

AChE inhibitors are an effective for treatment of AChR-MG symptoms, but may cause muscle cramps, fasciculation, dysphagia, and respiratory insufficiency in MuSK-MG patients.[14,36] Therefore, to investigate the effect of AChE-inhibition on recovery of neuromuscular transmission, we administered the AChE inhibitor neostigmine to MuSK-injected mice, and recorded CMAPs by repetitive nerve stimulation before and 20 minutes after neostigmine administration (37.5 μg/kg). Although all neostigmine-treated, MuSK-injected mice (n = 6) exhibited a significant reversal in CMAP decline, only one mouse recovered CMAP to within 10% of the decline (9.2%), which is considered a normal response (Figure 6, A and B). Of note, in two neostigmine-treated, MuSK-injected mice, we recorded an abnormal EMG pattern 5 to 20 ms after the CMAP peak in the first trace in a stimulation series, as is observed in MuSK-MG patients after AChE inhibitor treatment (Figure 6C).[37,38] Furthermore, another abnormal EMG pattern related to a congenital myasthenic syndrome caused by an AChE deficiency was recorded in a separate MuSK-injected mouse (Figure 6D).[39] Repetitive nerve stimulation at 3 Hz elicited a second CMAP with smaller amplitude than the first, a moderate decline of the primary CMAP, and a faster decline of the secondary CMAP. We did not observe abnormal EMG patterns after neostigmine injection in control mice (data not shown). These observations indicate abnormal sensitivities to ACh at endplates after MuSK injection, and suggest that the pathological conditions of patients with neuromuscular disorders could be reproduced in MuSK-injected mice.

Given that abnormal electrophysiological signs have been observed in MuSK-MG patients administered an overdose of AChE inhibitors or in patients with congenital myasthenia with AChE deficiency,[38,39] we postulated that AChE deficiency relative to ACh activity at NMJs might be the cause of these abnormalities. We therefore examined the expression of AChE and the AChE-anchoring protein ColQ, which may bind to MuSK and promote the accumulation of AChE at the postsynaptic membrane.[40,41] Using BTx and antibodies against AChE and ColQ, we triple-labeled soleus muscle whole mounts from MuSK-injected and control mice. The intensities of both AChE and ColQ expression at NMJs in MuSK-injected mice were reduced (Figure 6E), and the area of AChE expression was decreased significantly in MuSK-injected mice (n = 104 NMJs in 3 mice), compared with control mice (n = 91 NMJs in 3 mice) (Figure 6, E and F).

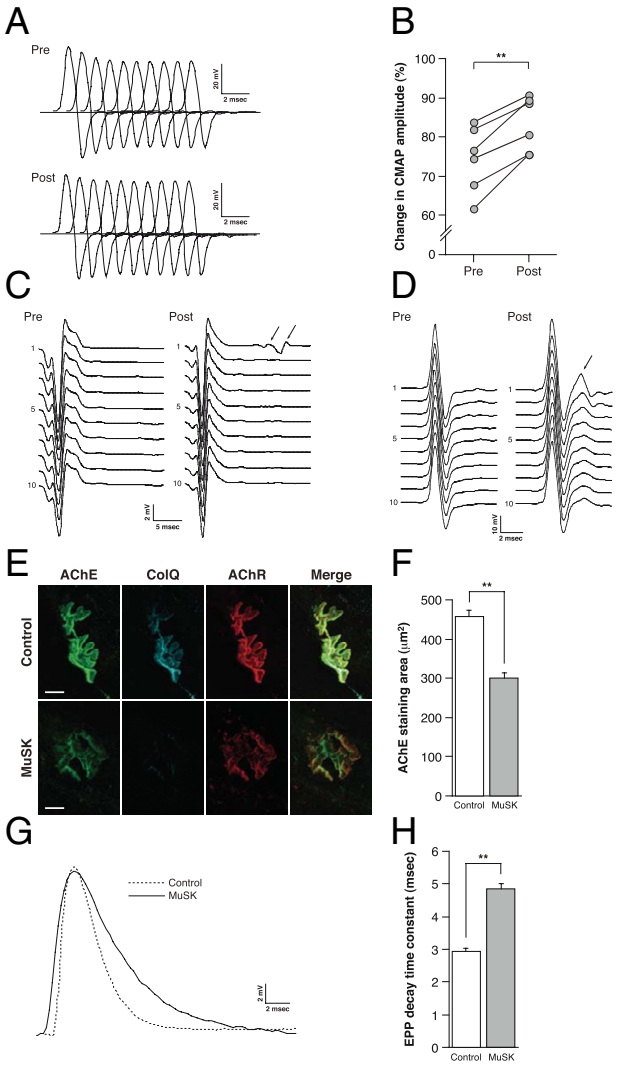

Figure 6. Impairment of AChE function in MuSK-injected mice. **A:** Representative EMG traces before and after neostigmine treatment. **B:** Neostigmine induced a significant reversal of CMAP decrement, ranging from 23.4% to 54.1% (mean, 36.4 ± 4.8%). $^{**}P < 0.01$ (paired *t*-test). **C** and **D:** Abnormal EMG traces evoked by neostigmine treatment. After neostigmine treatment, disturbance of baseline (**arrows**) after CMAP emerged in the first trace only (**C**), and a second CMAP (**arrow**) emerged, with smaller amplitude than the first, and then gradually disappeared (**D**). **E:** Levels of antibody staining for AChE (green), ColQ (cyan), and Alexa Fluor 647-BTx labeling of AChRs (red) were reduced in soleus muscles of MuSK-injected mice, compared with controls. Scale bars: 10 μm. **F:** The average AChE staining area decreased to 65.8% of control values in MuSK-injected mice; ≥30 NMJs from each mouse (n = 3 mice/group) were quantified. **G:** Representative EPP traces from control and MuSK-injected mouse diaphragms. In EPP traces with equivalent amplitudes, MuSK-injected mice exhibited longer EPP decay time constants (τ = 5.0 ms), compared with controls (τ = 2.6 ms). **H:** The mean EPP τ of MuSK-injected mice was 164% that of control mice. Data are expressed as means ± SEM from ≥10 NMJs of each mouse (n = 3 mice/group). $^{**}P < 0.01$ versus control mice (*t*-test).

Furthermore, we investigated the impairment of AChE function by examining the rate of EPP decay, the EPP decay time constant (τ), using intracellular recordings as described above.[42] In traces with similar amplitudes, the falling phase of the EPP of MuSK-injected mice was not as steep as that of controls (Figure 6G), and the mean EPP τ of MuSK-injected mice (4.85 ± 0.16 ms, n = 30 NMJs in 3 mice) was longer than that of controls (2.95 ± 0.07 ms, n = 53 NMJs in 3 mice) (Figure 6H), indicating that the AChE at NMJs in MuSK-injected mice could not hydrolyze ACh rapidly, leading to prolonged ACh action. Taken together, our results demonstrate that MuSK is required for the binding of AChE clusters to ColQ at the NMJ postsynaptic membrane *in vivo* and that MuSK Abs interfered with AChE function, leading to hypersensitivity to ACh after neostigmine treatment.

Discussion

In the present study, we investigated the pathophysiology of MuSK-MG using a new animal model in which 100% of mice synchronously develop MG after MuSK protein injection. In addition, we demonstrated the pathogenicity of MuSK Abs and found novel roles for MuSK activity at mature NMJs.

We previously demonstrated the pathogenicity of MuSK Abs via active immunization of rabbits with recombinant soluble MuSK protein.[7] In addition, EAMG induced by inoculation of MuSK protein has also been successfully established in mice.[23,43] Furthermore, when passive transfer of human MuSK Abs from MG patients into mice caused severe muscle weakness,[8] and EMG results were compatible with a diagnosis of MG, the pathogenicity of MuSK Abs was confirmed. Although it has been postulated that the human IgG4 subclass of autoantibodies causes MuSK-MG without complement activation, previous pathophysiological studies did not include complement-deficient animals.[9,10,44]

The A/WySnJ mouse strain cannot generate the membrane attack complex, which is the cytolytic end product of the complement cascade, because of mutations in the complement component 5 gene (*C5*).[19] Thus, the use of this strain allowed us to completely eliminate the role of complement activation on the onset of MG and to analyze non-complement-mediated effects. Previously, a high incidence of EAMG after MuSK immunization was also observed in A/J mice, which exhibit the same C5 deficiency as A/WySnJ mice.[23] We demonstrated that not only A/J but also other C5-deficient strains exhibited a severe form of MuSK-EAMG at a high incidence, as observed in the A/WySnJ strain. Complement-mediated damage to postsynaptic membranes is considered to be the major pathogenic mechanism in AChR-MG, because complement-deficient mice are resistant to EAMG induced by AChR immunization.[20,21] However, our results demonstrate that complement activation is not necessary for the onset of MuSK-MG, and provide insight into the mechanism by which the IgG4 subclass of MuSK Abs causes human MG.[9,10]

The IgG4 subclass of MuSK Abs observed in MG patients may have a functionally monovalent antigen-binding site, because IgG4 exchanges Fab arms with non-pathogenic IgG4 *in vivo*.[45] Therefore, this particular IgG4 may not efficiently reduce the number of MuSK molecules on the surface of postsynaptic membranes by invoking a cross-linking mechanism requiring divalent antibodies. Although no dynamic exchange of the IgG-Fab arm is found in mouse IgG subclasses, we demonstrated *in*

vitro that the monovalent Fab fragments of MuSK-IgG inhibited MuSK signaling and AChR clustering. Therefore, MuSK antibody binding could directly inhibit MuSK function required for the maintenance of mature NMJs, as well as internalization of MuSK molecules from the plasma membrane.[7,46]

In the present study, we demonstrated that MuSK is required for maintenance of mature NMJ structure and function. Our complement-deficient mouse model exhibited a loss of AChR expression, as well as a reduction in the size of motor terminals apposing AChR clusters at NMJs. These changes were consistent with those observed in complement-sufficient animals that developed MuSK-EAMG[7,8,23,43] and in mice bearing the MuSK mutations observed in congenital myasthenic syndrome.[47,48] Furthermore, our ultrastructural studies indicate a significant loss of complexity in convoluted postsynaptic structures (eg, the flattening of synaptic gutters), as well as a decrease in the number of slit-like junctional folds at postsynaptic membranes.

In addition to morphological defects, our model exhibited functional defects at presynapses, including lower levels of transmitter release from nerve terminals. In clinical studies, low levels of presynaptic ACh release were found at NMJs of a MuSK-MG patient using *in vitro* electrophysiology, which is consistent with our results.[49,50] It has been shown that AChR-MG, which is caused exclusively by postsynaptic defects, results in an increase in quantal content in both patients and EAMG model animals, suggesting the involvement of a compensatory retrograde signaling mechanism between postsynaptic and presynaptic sites.[51,52] Therefore, the decrease in quantal content in MuSK-MG might imply dysfunction of this compensatory mechanism, suggesting that MuSK mediates retrograde signaling involving transmitter release from nerve terminals. In this regard, mice that carry an inactivated form of the gene encoding muscle-specific β-catenin, a signaling protein downstream of disheveled (Dvl), or laminin β2, also have morphological defects both presynaptically and postsynaptically.[31,32] These data point to the important roles these molecules play in NMJ formation. Furthermore, both spontaneous and evoked ACh release from nerve terminals are reduced by abnormalities in the vesicle release machinery or reductions in the number of release sites. Therefore, we cannot exclude the possibility that the defects observed in our EAMG model might result from impairment of the presynaptic component itself, via dysfunction of MuSK (although it is generally assumed that the reductions observed in presynaptic and postsynaptic areas are related to diminished ACh release[17]). Our data suggest that MuSK plays a role in the maintenance of presynaptic function at NMJs through retrograde signaling.

We demonstrated that MuSK is required for proper AChE function at NMJs and determined the mechanism by which AChE inhibitor treatment exacerbates MuSK-MG symptoms. It is clear that MuSK participates in the accumulation of AChE in the synaptic basal lamina of NMJs, possibly by forming complexes with ColQ, as postulated previously based on *in vitro* experiments.[41] MuSK might act as a scaffold molecule, anchoring those complexes to the synaptic basal lamina. Additionally, MuSK signaling may be required for the highly localized expression of AChE mRNA at mature NMJs.[53,54] Accumulated AChE in the synaptic cleft may tightly limit both the temporal and spatial extent of cholinergic neurotransmission by rapid cleavage of ACh at the basal lamina. However, inhibition of MuSK by MuSK Abs decreased levels of AChE at the basal lamina and impaired its function, as shown by the prolonged EPP time constant we observed. If AChE inhibitors were to be administered in these conditions, the rebinding to AChRs by an excess of ACh existing at the synaptic cleft could provoke cholinergic hypersensitivity (recorded as an abnormal EMG pattern) and so could eventually lead to cholinergic crises.

Clinically, MuSK-MG patients tend to have severely weak, atrophied muscles and are more refractory to treatment than AChR-MG patients. These differences in clinical symptoms between MuSK-MG and AChR-MG could result from the distinct pathogenic mechanisms involved in these two types of MG. Overall, our results indicate that MuSK plays indispensable roles in the structural and functional maintenance of mature NMJs, and that disruption of MuSK function by specific autoantibodies causes MG (Figure 7). One of the main signals that cause advancement from presynapse to postsynapse stages is the agrin/MuSK pathway, but the retrograde signals regulated by MuSK are still elusive. Although fibroblast growth factors, laminin β2, and collagen α(IV) chains act as muscle-derived organizers of presynaptic differentiation, whether they act in conjunction with MuSK signaling is uncertain.[55,56] Our model of MuSK-MG did not exhibit immune complex-mediated damage to tissue that would otherwise participate in this interaction. Our model thus provides a valuable platform from which to evaluate the role of MuSK signaling in NMJ maintenance and the immune mechanisms and pathophysiology of MuSK-MG.

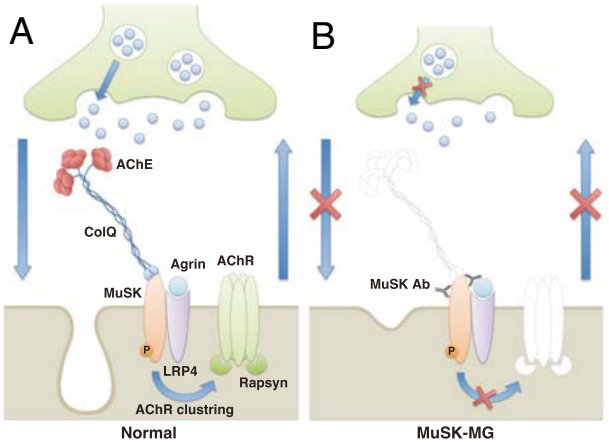

Figure 7. Pathogenic mechanism of MG induced by MuSK Abs. **A:** In normal NMJs, agrin binds to LRP4 to activate MuSK. MuSK regulates the maintenance of both presynaptic and postsynaptic structures and functions bidirectionally. **B:** MuSK Abs bind to the ectodomain of MuSK, causing MuSK degradation by antigenic modulation and/or direct inhibition of MuSK function. This inhibits MuSK, resulting in structural disruptions (eg, dispersal of AChR clusters, loss of synaptic folds, and degeneration of nerve terminals) and functional abnormalities (eg, decrease in ACh release) that eventually lead to MG. Furthermore, the decreased levels of AChE, which is anchored to MuSK by ColQ, can induce a cholinergic crisis mediated by AChE inhibitors, exacerbating the symptoms of MG.

As a result, this model could be instrumental in the development of effective medications for this group of devastating diseases.

Acknowledgments

We thank Terrone L. Rosenberry for AChE antibody and Fumio Hasegawa for excellent technical assistance with ultrastructural studies.

References

1. Vincent A, Lang B, Kleopa KA: Autoimmune channelopathies and related neurological disorders. Neuron 2006, 52:123–138
2. Conti-Fine BM, Milani M, Kaminski HJ: Myasthenia gravis: past, present, and future. J Clin Invest 2006, 116:2843–2854
3. Hoch W, McConville J, Helms S, Newsom-Davis J, Melms A, Vincent A: Auto-antibodies to the receptor tyrosine kinase MuSK in patients with myasthenia gravis without acetylcholine receptor antibodies. Nat Med 2001, 7:365–368
4. DeChiara TM, Bowen DC, Valenzuela DM, Simmons MV, Poueymirou WT, Thomas S, Kinetz E, Compton DL, Rojas E, Park JS, Smith C, DiStefano PS, Glass DJ, Burden SJ, Yancopoulos GD: The receptor tyrosine kinase MuSK is required for neuromuscular junction formation in vivo. Cell 1996, 85:501–512
5. Kim N, Stiegler AL, Cameron TO, Hallock PT, Gomez AM, Huang JH, Hubbard SR, Dustin ML, Burden SJ: Lrp4 is a receptor for agrin and forms a complex with MuSK. Cell 2008, 135:334–342
6. Zhang B, Luo S, Wang Q, Suzuki T, Xiong WC, Mei L: LRP4 serves as a coreceptor of agrin. Neuron 2008, 60:285–297
7. Shigemoto K, Kubo S, Maruyama N, Hato N, Yamada H, Jie C, Kobayashi N, Mominoki K, Abe Y, Ueda N, Matsuda S: Induction of myasthenia by immunization against muscle-specific kinase. J Clin Invest 2006, 116:1016–1024
8. Cole RN, Reddel SW, Gervasio OL, Phillips WD: Anti-MuSK patient antibodies disrupt the mouse neuromuscular junction. Ann Neurol 2008, 63:782–789
9. McConville J, Farrugia ME, Beeson D, Kishore U, Metcalfe R, Newsom-Davis J, Vincent A: Detection and characterization of MuSK antibodies in seronegative myasthenia gravis. Ann Neurol 2004, 55: 580–584
10. Ohta K, Shigemoto K, Fujinami A, Maruyama N, Konishi T, Ohta M: Clinical and experimental features of MuSK antibody positive MG in Japan. Eur J Neurol 2007, 14:1029–1034
11. Leite MI, Jacob S, Viegas S, Cossins J, Clover L, Morgan BP, Beeson D, Willcox N, Vincent A: IgG1 antibodies to acetylcholine receptors in 'seronegative' myasthenia gravis. Brain 2008, 131:1940–1952
12. Sanders DB, El-Salem K, Massey JM, McConville J, Vincent A: Clinical aspects of MuSK antibody positive seronegative MG. Neurology 2003, 60:1978–1980
13. Oh SJ: Muscle-specific receptor tyrosine kinase antibody positive myasthenia gravis current status. J Clin Neurol 2009, 5:53–64
14. Hatanaka Y, Hemmi S, Morgan MB, Scheufele ML, Claussen GC, Wolfe GI, Oh SJ: Nonresponsiveness to anticholinesterase agents in patients with MuSK-antibody-positive MG. Neurology 2005, 65:1508–1509
15. Tierney ML, Osborn KE, Milburn PJ, Stowell MH, Howitt SM: Phylogenetic conservation of disulfide-linked, dimeric acetylcholine receptor pentamers in southern ocean electric rays. J Exp Biol 2004, 207:3581–3590
16. Martin AR: A further study of the statistical composition on the end-plate potential. J Physiol 1955, 130:114–122
17. Wood SJ, Slater CR: Safety factor at the neuromuscular junction. Prog Neurobiol 2001, 64:393–429
18. Ezaki T, Oki S, Matsuda Y, Desaki J: Age changes of neuromuscular junctions in the extensor digitorum longus muscle of spontaneous thymoma BUF/Mna rats. A scanning and transmission electron microscopic study. Virchows Arch 2000, 437:388–395
19. Wetsel RA, Fleischer DT, Haviland DL: Deficiency of the murine fifth complement component (C5). A 2-base pair gene deletion in a 5′-exon. J Biol Chem 1990, 265:2435–2440
20. Christadoss P, Lindstrom JM, Talal N, Duvic CR, Kalantri A, Shenoy M: Immune response gene control of lymphocyte proliferation induced by acetylcholine receptor-specific helper factor derived from lymphocytes of myasthenic mice. J Immunol 1986, 137:1845–1849
21. Christadoss P, Tüzün E, Li J, Saini SS, Yang H: Classical complement pathway in experimental autoimmune myasthenia gravis pathogenesis. Ann N Y Acad Sci 2008, 1132:210–219
22. Stevens TL, Bossie A, Sanders VM, Fernandez-Botran R, Coffman RL, Mosmann TR, Vitetta ES: Regulation of antibody isotype secretion by subsets of antigen-specific helper T cells. Nature 1988, 334:255–258
23. Jha S, Xu K, Maruta T, Oshima M, Mosier DR, Atassi MZ, Hoch W: Myasthenia gravis induced in mice by immunization with the recombinant extracellular domain of rat muscle-specific kinase (MuSK). J Neuroimmunol 2006, 175:107–117
24. Xu K, Jha S, Hoch W, Dryer SE: Delayed synapsing muscles are more severely affected in an experimental model of MuSK-induced myasthenia gravis. Neuroscience 2006, 143:655–659
25. Valenzuela DM, Stitt TN, DiStefano PS, Rojas E, Mattsson K, Compton DL, Nuñez L, Park JS, Stark JL, Gies DR, Thomas S, Le Beau MM, Fernald AA, Copeland NG, Jenkins NA, Burden SJ, Glass DJ, Yancopoulos GD: Receptor tyrosine kinase specific for the skeletal muscle lineage: expression in embryonic muscle, at the neuromuscular junction, and after injury. Neuron 1995, 15:573–584
26. Engel AG, Tsujihata M, Lambert EH, Lindstrom JM, Lennon VA: Experimental autoimmune myasthenia gravis: a sequential and quantitative study of the neuromuscular junction ultrastructure and electrophysiologic correlations. J Neuropathol Exp Neurol 1976, 35:569–587
27. Glass DJ, Bowen DC, Stitt TN, Radziejewski C, Bruno J, Ryan TE, Gies DR, Shah S, Mattsson K, Burden SJ, DiStefano PS, Valenzuela DM, DeChiara TM, Yancopoulos GD: Agrin acts via a MuSK receptor complex. Cell 1996, 85:513–523
28. Hopf C, Hoch W: Dimerization of the muscle-specific kinase induces tyrosine phosphorylation of acetylcholine receptors and their aggregation on the surface of myotubes. J Biol Chem 1998, 273:6467–6473
29. Magleby KL: Neuromuscular transmission. Myology, ed 3. Edited by AG Engel, C Franzini-Armstrong. New York, McGraw-Hill, Medical Publishing Division, 2004, pp 373–396
30. Slater CR, Fawcett PR, Walls TJ, Lyons PR, Bailey SJ, Beeson D, Young C, Gardner-Medwin D: Pre- and post-synaptic abnormalities associated with impaired neuromuscular transmission in a group of patients with 'limb-girdle myasthenia'. Brain 2006, 129:2061–2076
31. Knight D, Tolley LK, Kim DK, Lavidis NA, Noakes PG: Functional analysis of neurotransmission at beta2-laminin deficient terminals. J Physiol 2003, 546:789–800
32. Li XM, Dong XP, Luo SW, Zhang B, Lee DH, Ting AK, Neiswender H, Kim CH, Carpenter-Hyland E, Gao TM, Xiong WC, Mei L: Retrograde regulation of motoneuron differentiation by muscle beta-catenin. Nat Neurosci 2008, 11:262–268
33. Thompson JS, Bixler SA, Qian F, Vora K, Scott ML, Cachero TG, Hession C, Schneider P, Sizing ID, Mullen C, Strauch K, Zafari M, Benjamin CD, Tschopp J, Browning JL, Ambrose C: BAFF-R, a newly identified TNF receptor that specifically interacts with BAFF. Science 2001, 293:2108–2111
34. Mayne CG, Amanna IJ, Nashold FE, Hayes CE: Systemic autoimmunity in BAFF-R-mutant A/WySnJ strain mice. Eur J Immunol 2008, 38:587–598
35. Tüzün E, Scott BG, Goluszko E, Higgs S, Christadoss P: Genetic evidence for involvement of classical complement pathway in induction of experimental autoimmune myasthenia gravis. J Immunol 2003, 171:3847–3854
36. Punga AR, Stålberg E: Acetylcholinesterase inhibitors in MG: to be or not to be? Muscle Nerve 2009, 39:724–728
37. Punga AR, Flink R, Askmark H, Stålberg EV: Cholinergic neuromuscular hyperactivity in patients with myasthenia gravis seropositive for MuSK antibody. Muscle Nerve 2006, 34:111–115
38. Punga AR, Sawada M, Stålberg EV: Electrophysiological signs and the prevalence of adverse effects of acetylcholinesterase inhibitors in patients with myasthenia gravis. Muscle Nerve 2008, 37:300–307
39. Bestue-Cardiel M, Sáenz de Cabezón-Alvarez A, Capablo-Liesa JL, López-Pisón J, Peña-Segura JL, Martin-Martinez J, Engel AG: Con-

genital endplate acetylcholinesterase deficiency responsive to ephedrine. Neurology 2005, 65:144–146
40. Feng G, Krejci E, Molgó J, Cunningham JM, Massoulié J, Sanes JR: Genetic analysis of collagen Q: roles in acetylcholinesterase and butyrylcholinesterase assembly and in synaptic structure and function. J Cell Biol 1999, 144:1349–1360
41. Cartaud A, Strochlic L, Guerra M, Blanchard B, Lambergeon M, Krejci E, Cartaud J, Legay C: MuSK is required for anchoring acetylcholinesterase at the neuromuscular junction. J Cell Biol 2004, 165:505–515
42. Kohara N, Lin TS, Fukudome T, Kimura J, Sakamoto T, Kaji R, Shibasaki H: Pathophysiology of weakness in a patient with congenital end-plate acetylcholinesterase deficiency. Muscle Nerve 2002, 25: 585–592
43. Shigemoto K, Kubo S, Jie C, Hato N, Abe Y, Ueda N, Kobayashi N, Kameda K, Mominoki K, Miyazawa A, Ishigami A, Matsuda S, Maruyama N: Myasthenia gravis experimentally induced with muscle-specific kinase. Ann N Y Acad Sci 2008, 1132:93–98
44. Niks EH, van Leeuwen Y, Leite MI, Dekker FW, Wintzen AR, Wirtz PW, Vincent A, van Tol MJ, Jol-van der Zijde CM, Verschuuren JJ: Clinical fluctuations in MuSK myasthenia gravis are related to antigen-specific IgG4 instead of IgG1. J Neuroimmunol 2008, 195:151–156
45. van der Neut Kolfschoten M, Schuurman J, Losen M, Bleeker WK, Martinez-Martinez P, Vermeulen E, den Bleker TH, Wiegman L, Vink T, Aarden LA, De Baets MH, van de Winkel JG, Aalberse RC, Parren PW: Anti-inflammatory activity of human IgG4 antibodies by dynamic Fab arm exchange. Science 2007, 317:1554–1557
46. Cole RN, Ghazanfari N, Ngo ST, Gervásio OL, Reddel SW, Phillips WD: Patient autoantibodies deplete postsynaptic muscle specific kinase leading to disassembly of the ACh receptor scaffold and myasthenia gravis in mice. J Physiol 2010, 588:3217–3229
47. Chevessier F, Faraut B, Ravel-Chapuis A, Richard P, Gaudon K, Bauche S, Prioleau C, Herbst R, Goillot E, Ioos C, Azulay JP, Attarian S, Leroy JP, Fournier E, Legay C, Schaeffer L, Koenig J, Fardeau M, Eymard B, Pouget J, Hantaï D: MUSK, a new target for mutations causing congenital myasthenic syndrome. Hum Mol Genet 2004, 13:3229–3240
48. Chevessier F, Girard E, Molgó J, Bartling S, Koenig J, Hantaï D, Witzemann V: A mouse model for congenital myasthenic syndrome due to MuSK mutations reveals defects in structure and function of neuromuscular junctions. Hum Mol Genet 2008, 17:3577–3595
49. Burges J, Vincent A, Molenaar PC, Newsom-Davis J, Peers C, Wray D: Passive transfer of seronegative myasthenia gravis to mice. Muscle Nerve 1994, 17:1393–1400
50. Niks EH, Kuks JB, Wokke JH, Veldman H, Bakker E, Verschuuren JJ, Plomp JJ: Pre- and postsynaptic neuromuscular junction abnormalities in musk myasthenia. Muscle Nerve 2010, 42:283–288
51. Plomp JJ, Van Kempen GT, De Baets MB, Graus YM, Kuks JB, Molenaar PC: Acetylcholine release in myasthenia gravis: regulation at single end-plate level. Ann Neurol 1995, 37:627–636
52. Cull-Candy SG, Miledi R, Trautmann A, Uchitel OD: On the release of transmitter at normal, myasthenia gravis and myasthenic syndrome affected human end-plates. J Physiol 1980, 299:621–638
53. Jasmin BJ, Lee RK, Rotundo RL: Compartmentalization of acetylcholinesterase mRNA and enzyme at the vertebrate neuromuscular junction. Neuron 1993, 11:467–477
54. Legay C, Huchet M, Massoulié J, Changeux JP: Developmental regulation of acetylcholinesterase transcripts in the mouse diaphragm: alternative splicing and focalization. Eur J Neurosci 1995, 7:1803–1809
55. Fox MA, Sanes JR, Borza DB, Eswarakumar VP, Fässler R, Hudson BG, John SW, Ninomiya Y, Pedchenko V, Pfaff SL, Rheault MN, Sado Y, Segal Y, Werle MJ, Umemori H: Distinct target-derived signals organize formation, maturation, and maintenance of motor nerve terminals. Cell 2007, 129:179–193
56. Nishimune H, Sanes JR, Carlson SS: A synaptic laminin-calcium channel interaction organizes active zones in motor nerve terminals. Nature 2004, 432:580–587